

Ultimate behavior and ultimate load capacity of steel cable-stayed bridges

D. H. Choi[†], H. Yoo[‡], J. I. Shin^{††} and S. I. Park^{††}

*Department of Civil Engineering, Hanyang University, 17 Haengdang-dong,
Seoungdong-gu, Seoul 133-791, Korea*

K. Nogami^{†††}

*Department of Civil Engineering, Tokyo Metropolitan University, 1-1 Minami-osawa, Hachioji-shi,
Tokyo 192-0397, Japan*

(Received September 1, 2006, Accepted August 1, 2007)

Abstract. The main purpose of this paper is to investigate the ultimate behavior of steel cable-stayed bridges with design variables and compare the validity and applicability of computational methods for evaluating ultimate load capacity of cable-stayed bridges. The methods considered in this paper are elastic buckling analysis, inelastic buckling analysis and nonlinear elasto-plastic analysis. Elastic buckling analysis uses a numerical eigenvalue calculation without considering geometric nonlinearities of cable-stayed bridges and the inelastic material behavior of main components. Inelastic buckling analysis uses an iterative eigenvalue calculation to consider inelastic material behavior, but cannot consider geometric nonlinearities of cable-stayed bridges. The tangent modulus concept with the column strength curve prescribed in AASHTO LRFD is used to consider inelastic buckling behavior. Detailed procedures of inelastic buckling analysis are presented and corresponding computer codes were developed. In contrast, nonlinear elasto-plastic analysis uses an incremental-iterative method and can consider both geometric nonlinearities and inelastic material behavior of a cable-stayed bridge. Proprietary software ABAQUS are used and user-subroutines are newly written to update equivalent modulus of cables to consider geometric nonlinearity due to cable sags at each increment step. Ultimate load capacities with the three analyses are evaluated for numerical models of cable-stayed bridges that have center spans of 600 m, 900 m and 1200 m with different girder depths and live load cases. The results show that inelastic buckling analysis is an effective approximation method, as a simple and fast alternative, to obtain ultimate load capacity of long span cable-stayed bridges, whereas elastic buckling analysis greatly overestimates the overall stability of cable-stayed bridges.

Keywords: elastic buckling analysis; inelastic buckling analysis; nonlinear elasto-plastic analysis; ultimate load capacity; cable-stayed bridge.

[†] Ph.D., E-mail: samga@hanyang.ac.kr

[‡] Ph.D., Corresponding author, E-mail: csmile@hanyang.ac.kr

^{††} M.S., E-mail: joynina@nate.com

^{††} M.S., E-mail: psi8183@hanmail.net

^{†††} Ph.D., E-mail: nogami-kunie@c.metro.ac.jp

1. Introduction

Due to their aesthetic appearance, efficient utilization of structural materials and other notable advantages, cable-stayed bridges have gained much popularity in recent decades (Gimsing 1983, Poldony and Scalzi 1976). Since the construction of the first modern cable-stayed bridge, the Strömsund Bridge in Sweden in 1955, this kind of bridge has been used extensively for medium and long span crossings all over the world. The Tatara Grand Bridge (1999) in Japan, which is the longest cable-stayed bridge in the world, and two super-long bridges are now under design: the Sutong Bridge (China) and the Stonecutters Bridge (Hong Kong), showing the popularity of such bridges in Asia.

In this century, cable-stayed bridges have entered a new era, reaching central spans of 400 m to 1000 m and span lengths are still extending due to the development of computer technology, high strength steel cables and construction technology (Nagai *et al.* 2004, Xi and Kuang 1999, Wang 1999). In addition, the geometric shape of the main girders of cable-stayed bridges tends to be shallower and lighter in weight with the increasing central span of modern cable-stayed bridges (Ren 1999). Indeed, since the cables instead of the interval piers support these bridges, they are much more flexible than conventional continuous bridges, especially long span bridges. As a result, overall stability characteristics and ultimate behavior of cable-stayed bridges are more important and more complex. It is well known that cable-stayed bridges exhibit nonlinear behavior under normal design loads due to cable sag, combined axial force-bending moment interaction and large displacement (Wang *et al.* 2002, Shu and Wang 2001, Xi and Kuang 2000, George 1999). Furthermore, the near-collapse behavior of cable-stayed bridges is highly nonlinear (Adeli and Zhang 1995). Therefore, these nonlinearities should be taken into account in order to evaluate overall safety and ultimate load capacity of a cable-stayed bridge.

Overall stability and ultimate load capacity of cable-stayed bridges has historically been evaluated by the bifurcation stability theory. Tang (1976) first derived and calculated the buckling load of cable-stayed bridges using a simple energy method. Ermopoulos (1992) performed eigenvalue analysis on cable-stayed bridges to evaluate their overall safety. Wang (1999) investigated cable effects on the behavior of cable-stayed bridges using eigenvalue analysis. Similarly, Shu and Wang (2001) carried out stability analysis of box-girder cable-stayed bridges by eigenvalue analysis and investigated influences of design variables such as main span length, component stiffness and cable arrangement on overall load capacity. Although all of the reported results were meaningful and useful for the design of short or medium cable-stayed bridges, the method used in these studies cannot evaluate overall safety of long cable-stayed bridges precisely since eigenvalue analysis cannot handle geometric and material nonlinearities.

Researchers have become interested in the fully nonlinear analysis of cable-stayed bridges by finite element analysis as developing of the high performance of personal computers. Kanok-Nukulchai and Hong (1993) suggested nonlinear modeling techniques for girders and cables using the thin-walled element and special cable elements. Adeli and Zhang (1995) investigated the effect of geometric and material nonlinearities on ultimate load capacity and ultimate behavior of composite girder cable-stayed bridges. Ren (1999) also determined the overall safety of cable-stayed bridges by elasto-plastic analysis; he discovered that the geometric nonlinearity has a small effect on the bridge behavior than material nonlinearity. On the other side, Iwasaki *et al.* (2001) suggested the use of inelastic buckling analysis, which is a simple iterative method applying numerical eigenvalue calculation in order to avoid the difficulties of nonlinear elasto-plastic analysis. Recently, Nagai *et al.*

(2004) discussed the feasibility of the super-long steel cable-stayed bridge that has a center span of 1400 m by elasto-plastic analysis. Despite these insights, the effects of span length on the ultimate behavior of cable-stayed bridges must still be studied because super-long bridges that have the center span more than 1000 m will be in common in the near future. Furthermore, although nonlinear elasto-plastic analysis is the most accurate method, a simpler and faster approximate method is needed for evaluation of the ultimate load capacity of cable-stayed bridges since the rigorous nonlinear elasto-plastic analysis is too complex and time-consuming to use in practical design process.

The purpose of this paper is to investigate ultimate behavior with design variables such as center spans, girder depths and live load cases, and compare the validity and the applicability of computational methods for evaluation of ultimate load capacity of steel cable-stayed bridges. The ultimate load capacity of bridges is evaluated using elastic, inelastic and nonlinear elasto-plastic analyses. Parametric studies were performed in order to investigate the individual influence of such design variables on the ultimate load capacity of cable-stayed bridges. Because the general finite-element packages cannot handle the specific features of inelastic buckling analysis, corresponding computer codes for cable-stayed bridge analysis were developed for inelastic buckling analysis. In contrast, commercial codes, ABAQUS, were used in order to perform nonlinear elasto-plastic analysis with user-subroutines, which considers the sag nonlinearity of cables in cable-stayed bridges.

2. Evaluation methods of ultimate load capacity

2.1 Definition of ultimate load capacity for cable-stayed bridges

The stability of a structural system is lost due to singular points on the equilibrium path, referred to as critical points. There are two alternative concepts of overall structural stability: bifurcation stability and limit-load stability. Bifurcation stability is characterized by the fact that as the external load increases the system that originally deflected in the direction of the applied load suddenly deflects in a different direction. The critical load is commonly determined from an eigenvalue analysis of an idealized elastic model of the structure. On the other hand, limit-load stability is characterized by the fact that there is only a single mode of deflection from the start of loading to the limit or maximum load. The incremental-load analysis and load-displacement curve are needed in order to determine the critical load of system because the tangent stiffness of the system is indefinite at the critical load.

In this study, three methods are used in order to calculate ultimate load capacity of cable-stayed bridges. First, elastic buckling analysis is performed and the minimum eigenvalue of the first eigenmode is used as an indicator of ultimate load capacity. Second, inelastic buckling analysis is performed and a converged eigenvalue is used as an indicator of ultimate load capacity. Lastly, nonlinear elasto-plastic analysis is performed with ABAQUS and the critical load proportion factor (CLPF), that is determined at the peak point of load-displacement curve, is used as an indicator of ultimate load capacity. Elastic and inelastic buckling analyses are based on bifurcation stability, whereas nonlinear elasto-plastic analysis is based on limit-load stability. Table 1 contrasts indicators for ultimate load capacity of cable-stayed bridges with these methods.

Table 1 Comparison of indicators for the ultimate load capacity of cable-stayed bridges

The first eigenvalue, converged eigenvalue and load proportional factor			
Analysis method	Elastic buckling analysis	Inelastic buckling analysis	Nonlinear elasto-plastic analysis
Indicators for ultimate load capacity	κ_{\min} (Minimum eigenvalue)	κ_{\min}^{conv} (Converged eigenvalue)	CLPF (Critical Load Proportion Factor)

2.2 Elastic buckling analysis: Eigenvalue analysis

In bifurcation stability, structure is assumed to be a perfect structural system and to have elastic material behavior. The critical load is determined by a conventional eigenvalue calculation. The basic equation can be expressed as

$$([K_e] + \kappa[K_g])\{\phi\} = \{0\} \tag{1}$$

where $[K_e], [K_g]$ and $\{\phi\}$ are the elastic stiffness, geometric stiffness and buckling eigenmodes corresponding eigenvalues of κ , respectively. The stiffness matrix can be derived by using the concept of general continuum mechanics and the principle of virtual work (Yang and Kuo 1994, McGuire *et al.* 2000). Fig. 1 presents the 3-dimensional beam element and corresponding degrees of freedom. Moreover, Fig. 2 shows the elastic and geometric stiffness matrix for girders and towers in cable-stayed bridges explicitly used in this study. Since the geometric stiffness matrix is a function of element forces, a linear stress analysis is needed before performing elastic buckling analysis. The minimum eigenvalue of the first eigenmode is used as an indicator of ultimate load capacity of cable-stayed bridges.

2.3 Inelastic buckling analysis: iterative eigenvalue analysis

The tangent modulus theory proposed by Engesser (1889) is based on bifurcation stability and considers the inelastic behavior of a column as the tangent modulus, that is, the gradient at a specific point of the stress-strain curve. The inelastic buckling load P_{cr} can be written as

$$P_{cr} = \frac{\pi^2 E_t I}{l_e^2} = \frac{E_t}{E} P_e \tag{2}$$

where E_t, E, l_e and P_e are the tangent modulus, the modulus of elasticity, effective buckling length and the Euler buckling load $\pi^2 EI/l_e^2$, respectively. Eq. (2) can be transformed into

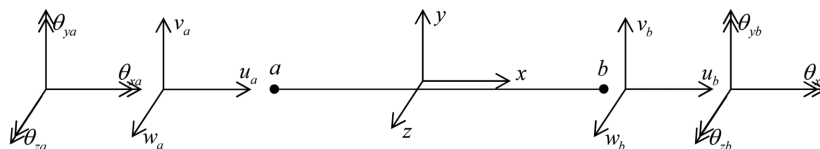


Fig. 1 3-dimensional beam element and its degrees of freedom

u_a	v_a	w_a	θ_{xa}	θ_{ya}	θ_{za}	u_b	v_b	w_b	θ_{xb}	θ_{yb}	θ_{zb}
a	0	0	0	0	0	$-a$	0	0	0	0	0
	b_z	0	0	0	c_z	0	$-b_z$	0	0	0	c_z
		b_y	0	$-c_y$	0	0	0	$-b_y$	0	$-c_y$	0
			d	0	0	0	0	0	$-d$	0	0
				e_y	0	0	0	c_y	0	f_y	0
					e_z	0	$-c_z$	0	0	0	f_z
						a	0	0	0	0	0
							b_z	0	0	0	$-c_z$
			Symm					b_y	0	c_y	0
									d	0	0
										e_y	0
											e_z

Where

$$a = EA/L, \quad b_y = 12EI_y/L^3, \quad b_z = 12EI_z/L^3, \\ c_y = 6EI_y/L^2, \quad c_z = 6EI_z/L^2, \\ d = GJ/L, \quad e_y = 4EI_y/L, \quad e_z = 4EI_z/L, \\ f_y = 2EI_y/L, \quad f_z = 2EI_z/L$$

(a) Elastic stiffness matrix

u_a	v_a	w_a	θ_{xa}	θ_{ya}	θ_{za}	u_b	v_b	w_b	θ_{xb}	θ_{yb}	θ_{zb}
a	0	0	0	0	0	$-a$	0	0	0	0	0
	b	0	c_{ya}		e	0	$-b$	0	c_{yb}	$-d$	e
		b	c_{za}	$-e$	d	0	0	$-b$	c_{zb}	$-e$	$-d$
			f	$-g_{za}$	g_{ya}	0	$-c_{ya}$	$-c_{za}$	$-f$	$-h_z$	h_y
				i	0	0	$-d$	e	$-h_z$	$-j$	k
					i	0	$-e$	$-d$	h_y	$-k$	$-j$
						a	0	0	0	0	0
							b	0	$-c_{yb}$	d	$-e$
			Symm					b	$-c_{zb}$	e	d
									f	g_{zb}	g_{yb}
										i	0
											i

Where

$$a = F/L, \quad b = 6F/(5L), \\ c_{ya} = M_{ya}/L, \quad c_{yb} = M_{yb}/L, \quad c_{za} = M_{za}/L, \\ c_{zb} = M_{zb}/L, \quad d = M_x/L, \quad e = F/10, \\ f = FJ/(AL), \\ g_{ya} = (2M_{ya} - M_{yb})/6, \quad g_{yb} = (M_{ya} - 2M_{yb})/6, \\ g_{za} = (2M_{za} - M_{zb})/6, \quad g_{zb} = (M_{za} - 2M_{zb})/6, \\ h_y = (M_{ya} + M_{yb})/6, \quad h_z = (M_{za} + M_{zb})/6, \\ i = 2FL/15, \quad j = FL/30, \quad k = M_x/2$$

(b) Geometric stiffness matrix

Fig. 2 The elastic and geometric stiffness for girder and tower

$$E_t = \frac{P_{cr}}{P_e} E = \frac{F_{cr}}{F_{cr,e}} E \quad (3)$$

where F_{cr} is the inelastic buckling stress of a column and $F_{cr,e}$ is the elastic buckling stress (the Euler buckling stress). According to Eq. (3), the tangent modulus of a column can be determined as in the ratio of the inelastic buckling stress to the elastic buckling stress, multiplied by the modulus of elasticity of a column. Therefore, the elastic stiffness matrix can be modified by introducing the tangent modulus of each element in order to consider the inelastic material behavior. The basic

equation of inelastic buckling analysis is described as

$$([K_e(E_t)] + \kappa[K_g])\{\phi\} = \{0\} \quad (4)$$

where $K_e(E_t)$ is the modified stiffness matrix which is a function of tangent modulus E_t .

The major task of inelastic buckling analysis is to determine the tangent modulus at each component in cable-stayed bridges. The elastic buckling stress $F_{cr,e}$ can be determined easily by using conventional eigenvalue calculations. However, the state of stress in each main component is unknown at the ultimate stage; thus the inelastic buckling stress F_{cr} and the tangent modulus E_t of each component cannot be determined. Consequently, an iterative scheme is needed in order to determine the inelastic buckling stress F_{cr} and the tangent modulus E_t of each component, simultaneously.

In this study, the inelastic buckling stress F_{cr} of each component is approximated using the column strength curve for compression members prescribed by the design specifications. In most design specifications for steel structures, the various strength curves of a column are provided considering effects of initial imperfections, residual stresses, section shapes, etc. The column strength curve in Load and Resistance Factor Design (AASHTO 2004) is defined as

$$F_{cr} = \begin{cases} \frac{0.877 \pi^2 E}{\lambda^2} & \text{when } \lambda \geq 1.5 \sqrt{\pi^2 E / F_y} \\ 0.658 \lambda^2 \left(\frac{F_y}{\pi^2 E} \right) F_y & \text{when } \lambda < 1.5 \sqrt{\pi^2 E / F_y} \end{cases} \quad (5)$$

where λ is a slenderness ratio and defined as Kl/r . Kl is an effective length and r is the radius of gyration of a column. F_y is yield strength of a column. Fig. 3 indicates the graphical shape of column strength curves prescribed in AASHTO LRFD specifications for that the yield strength of steel is 450 MPa.

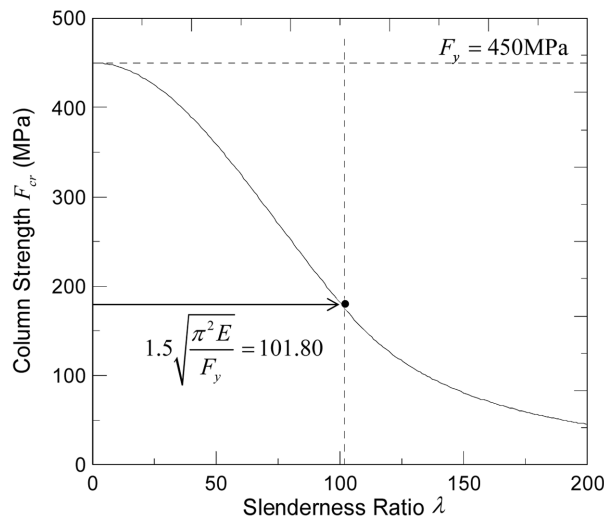


Fig. 3 The column strength curves for compression members in AASHTO specifications

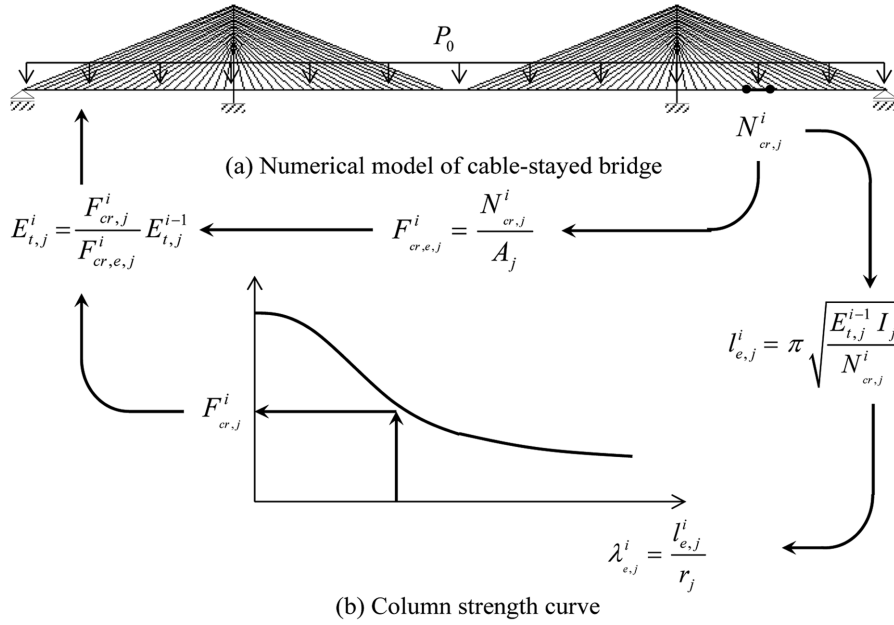


Fig. 4 Schematic diagram of inelastic buckling analysis

According to their states of stress, main components of cable-stayed bridges can be in a state of elastic buckling, inelastic buckling or yielding; thus they have a different modulus value. Based on the tangent modulus theory and an iterative scheme, the effective buckling length and the buckling load of each component can be determined by equalizing the elastic buckling stress $F_{cr,e}$ calculated from eigenvalue calculation with the buckling stress F_{cr} obtained from the column strength curve with effective buckling length. Namely, inelastic behavior of the main components of cable-stayed bridge can be approximated by using the column strength curve as a reference curve in inelastic buckling analysis. Fig. 4 presents schematic diagram of inelastic buckling analysis. In addition, a flow-chart for the computer program developed in this study is presented in Fig. 5. Finally, detailed procedures of inelastic buckling analysis are as follows:

- 1) Perform linear elastic finite element analysis for the numerical model of a cable-stayed bridge in order to calculate section forces in each element. Create elastic stiffness matrix $[K_e]$ and geometric stiffness matrix $[K_g]$ for the model.
- 2) Solve the eigenvalue problem designated as $|K_e(E_t^i) + \kappa[K_g(N)]| = 0$ and calculate the minimum eigenvalue κ_{min}^i . Calculate buckling load of each element as $N_{cr,j}^i = \kappa_{min}^i N_j$. Subscripts i and j are the number of iterations and the number of elements, respectively.
- 3) Calculate buckling stress of each element:
 - 3-a) Calculate the elastic buckling stress as $F_{cr,e,j}^i = N_{cr,j}^i / A_j$.
 - 3-b) Obtain the buckling stress $F_{cr,j}^i$ of each element from the column strength curve using effective buckling length of each element as $l_{e,j}^i = \pi \sqrt{E_{t,j}^{i-1} I_j / N_{cr,j}^i}$.
- 4) Calculate tangent modulus of each element as $E_{t,j}^i = \frac{F_{cr,j}^i}{F_{cr,e,j}^i} E_{t,j}^{i-1}$. Check for convergence with $F_{cr,e,j}^i$

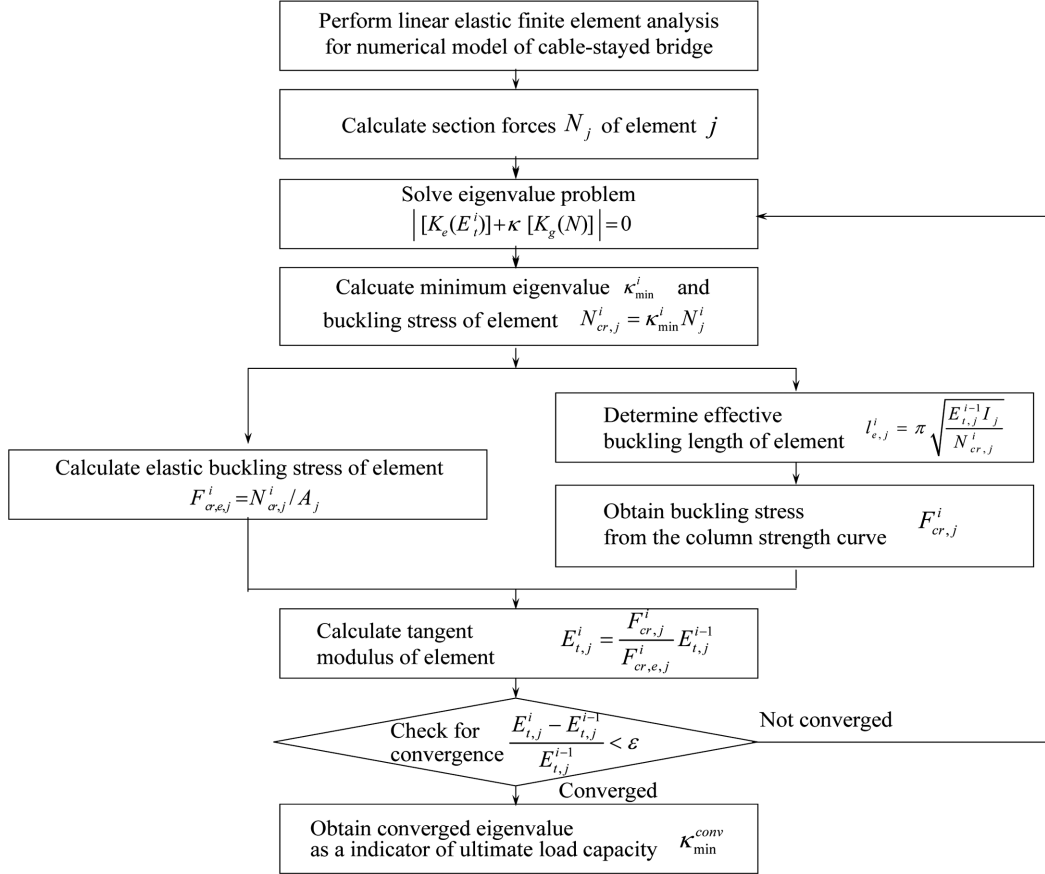


Fig. 5 Flow chart of inelastic buckling analysis

$\frac{E_{t,j}^i - E_{t,j}^{i-1}}{E_{t,j}^{i-1}} < \varepsilon$, where ε is the convergence limit (0.001). In case the convergence is not reached,

go back to procedure 2).

- 5) When convergence is satisfied, obtain the converged eigenvalue κ_{\min}^{conv} as an indicator of ultimate load capacity of a cable-stayed bridge.

In the procedures of inelastic buckling analysis, there may be some arguments about determination of the effective length of the girder and tower in cable-stayed bridges. The equation $N_{cr,j}^i = \kappa_{\min}^i N_j^i$ in the procedure 2) and $l_{e,j}^i = \pi \sqrt{E_{t,j}^{i-1} I_j / N_{cr,j}^i}$ in the procedure 3-b) imply that all members buckle simultaneously when the overall bridge is at the ultimate stage. Since all the members do not reach their individual buckling limits at the ultimate stage of the overall bridge, one cannot properly determine the effective length of all the members as described. However, these equations are used to calculate the tangent modulus with the procedure 4) in order to reflect the inelastic behavior of the members under ultimate loads, and may be used for the ultimate load capacity of a steel cable-stayed bridge.

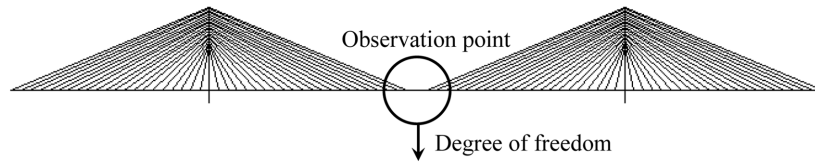


Fig. 6 The observation point for load-displacement curves

2.4 Nonlinear elasto-plastic analysis: Incremental-iterative analysis

Numerical models are analyzed by using proprietary software ABAQUS in order to determine the ultimate load capacity of cable-stayed bridges. In nonlinear elasto-plastic analysis with ABAQUS, equations of equilibrium are written in terms of deformed geometry based on the general finite deformation theory in order to accommodate geometric nonlinearities and material inelasticity of cable-stayed bridges. It is assumed that the deformations of the main components in cable-stayed bridges were characterized by large displacements, large rotations and small strains. Applied loads are divided into multiple load-increments. The modified Riks method with the Newton-Raphson iteration technique is applied for each load-increment in order to solve nonlinear equations. The critical load proportion factor can be determined by finding where the gradient of load-displacement curve is nearly zero, that is, the tangent stiffness of the overall structure becomes indefinite. The critical load proportion factor by nonlinear elasto-plastic analysis is compared to the minimum eigenvalue by elastic buckling analysis or converged eigenvalue by inelastic buckling analysis. The specific observation point is chosen at the center of main span of a cable-stayed bridge. For this observation point, the curves of load-displacement are plotted with a corresponding degree of freedom. Fig. 6 indicates the observation point and degree of freedom for plotting load-displacement curves.

The girders and towers of cable-stayed bridges are modeled by the two-node frame element, whereas the cables are modeled by the two-node bar element in ABAQUS. A peculiar nonlinearity occurs in the cables due to sag effect where the stiffness of the cables changes under the actions of dead load and axial tensile forces. On consideration of sag nonlinearity in inclined cable stays, it is convenient to use an equivalent straight cable element with an equivalent modulus of elasticity, which can well describe the catenary action of the cables. The concept of a cable equivalent modulus of elasticity was first introduced by Ernst (1965). If the change in tension in a cable during a load increment is not large, the axial stiffness of the cable will not change significantly and the equivalent modulus of elasticity of the cable is appropriate to consider cable sag nonlinearity during the load increment. The equivalent modulus of elasticity of the cable can be written as Eq. (6)

$$E_{eq} = \frac{E}{1 + \left[\frac{(wl_{ch})^2 AE}{12T^3} \right]} \tag{6}$$

where E_{eq} and E are the equivalent modulus of elasticity and the modulus of elasticity, respectively. w , A and T are unit weight of cables, area of cables and axial force of cables, respectively. Moreover, l_{ch} is a horizontal projected length of a cable.

Fig. 7 shows schematic procedures of user-subroutines in ABAQUS. Since the standard two-node bar element cannot handle the sag nonlinearity of cables, user subroutines USDFLD and URDFIL in ABAQUS are newly written for calculating the equivalent modulus with the axial force of each cable as Eq. (6). The user-subroutine USDFLD, which calculates the updated equivalent modulus, is called at the beginning of each load increment as shown in the revised Fig. 7. The initial cable forces should be used to estimate the initial equivalent modulus of cables at the start of the initial increment step using Eq. (6). Based on the field variables of the tension force (T) and the projective length (l_{ch}) of cables at the previous increment step, the equivalent modulus of each cable is computed subsequently. The amount of the load increment is set to be small enough to avoid the numerical problem. The equivalent modulus is re-evaluated in the beginning of each new load step,

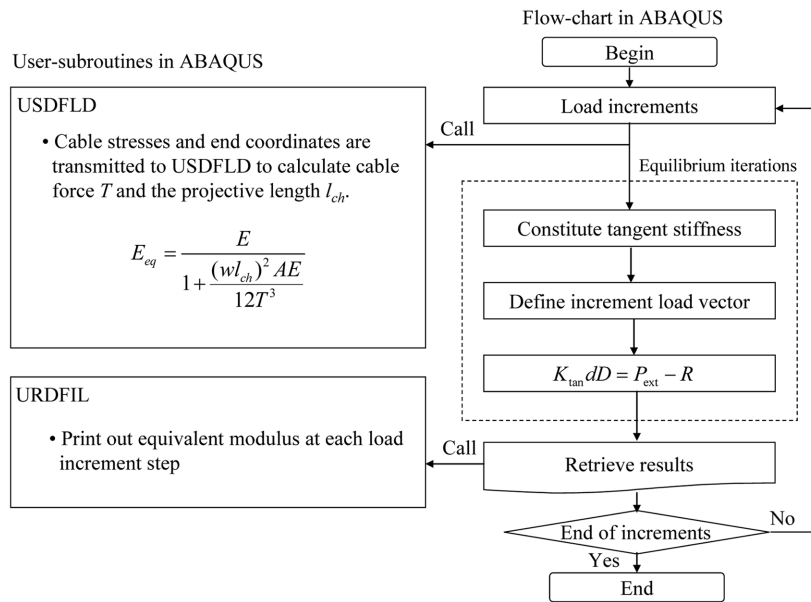


Fig. 7 Schematic procedure of user-subroutines in ABAQUS

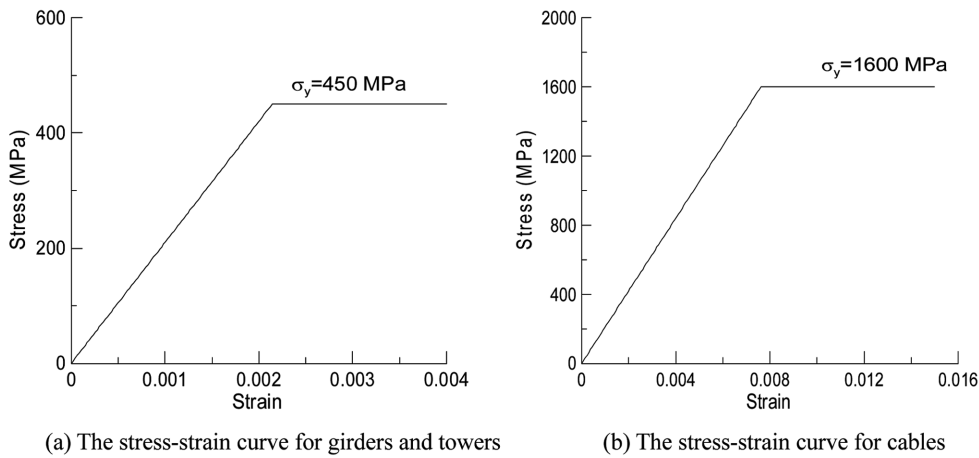


Fig. 8 Stress-strain characteristics of steel for components of a cable-stayed bridge

and remains unchanged throughout the process of the equilibrium iterations in the current increment step. After the equilibrium iterations are completed, the user-subroutine URDFIL is called in order to write out the results into the external file for user information. The above procedure is repeated until the structure reaches its ultimate stage with the load increment.

The ultimate load capacity also depends on the nonlinear stress-strain behavior of each component in cable-stayed bridges. In the incremental-iterative analysis procedure, the stiffness matrix of each component in local coordinates is revised into the elasto-plastic stiffness matrix when the stress of the integration points in each element exceeds the yield strength of the material. Fig. 8 presents elastic-perfectly plastic characteristics of stress-strain curve for girders, towers and cables used in this study.

3. Numerical models

3.1 Geometry

Cable-stayed bridges have three continuous girders and two towers. The towers are A-shaped and the cables are arranged as a fan type and fixed in the girders at 20-m intervals. The center spans of the cable-stayed bridges are 600 m, 900 m and 1200 m. The side span length is about half that of the center span. The ratio of tower height measured from the decks to center span is selected as one fifth.

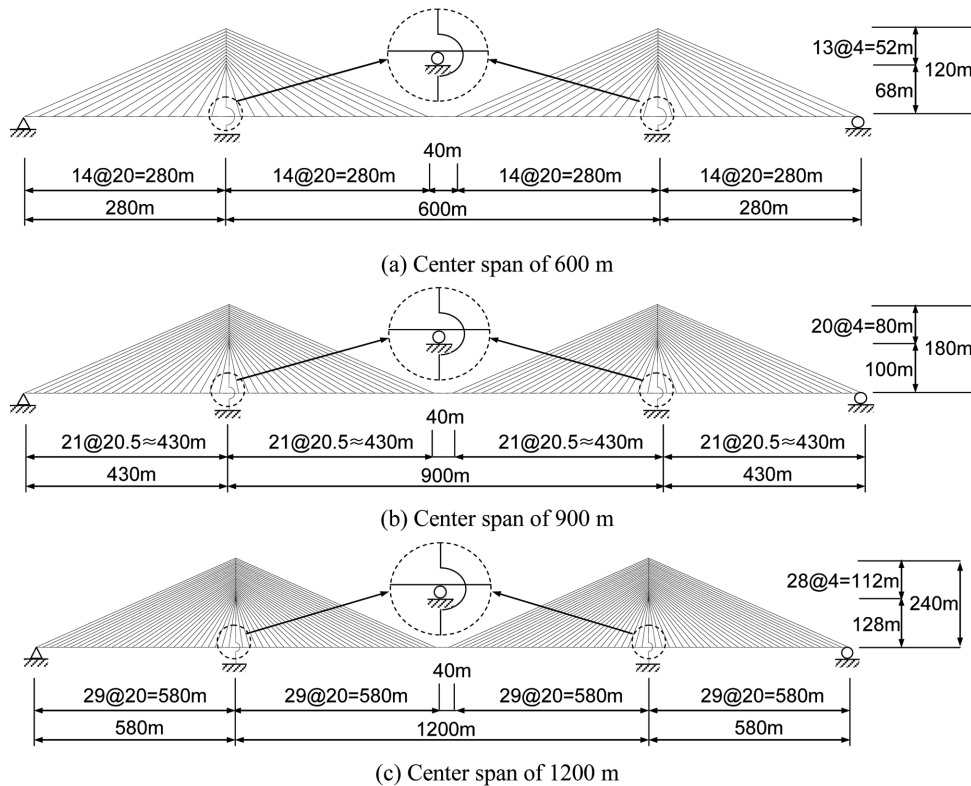


Fig. 9 Elevation of cable-stayed bridges

Fig. 9 presents the elevation view of all numerical models of cable-stayed bridges used in this study. Detailed geometric shapes of girders and towers are presented in Fig. 10 and information on sections is summarized in Table 2. The girders and towers are idealized as 4-cell boxes and 1-cell

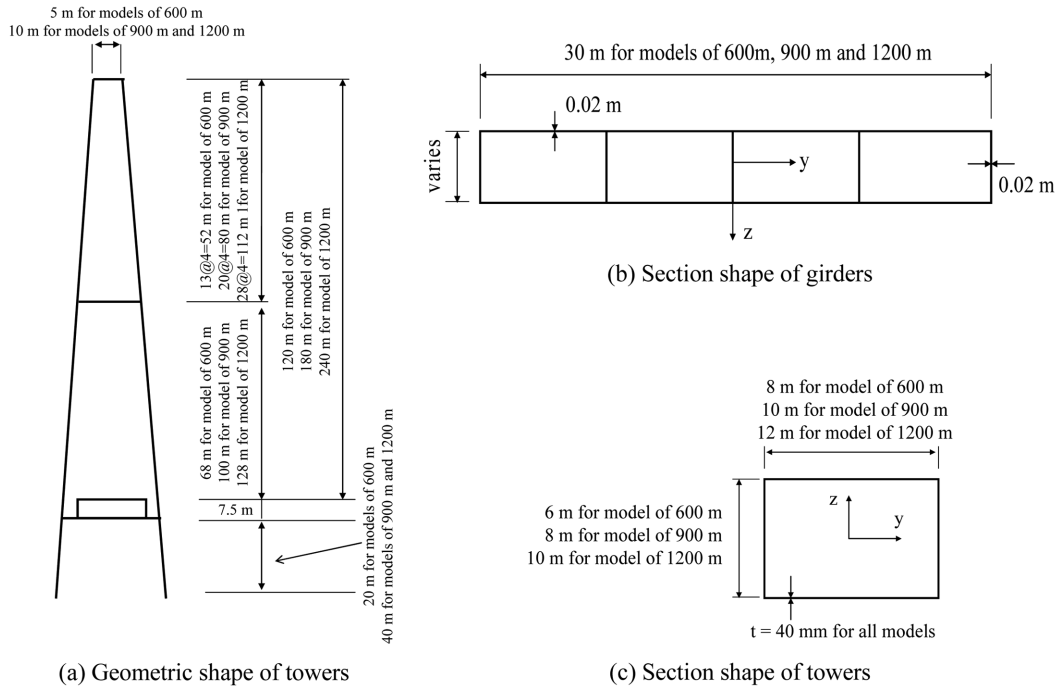


Fig. 10 Geometric shapes of girder and towers for cable-stayed bridges

Table 2 Information on sections of cable-stayed bridges

Model (width:m)	Girders					Material
	Depth H (m)	Area A (m ²)	Torsional const. J (m ⁴)	Moment of inertia I_y (m ⁴) I_z (m ⁴)		
600 m 900 m 1200 m (30 m)	1.0	1.296	1.115	0.296	100.786	$F_y = 450$ MPa $E = 2.1 \times 10^5$ MPa
	2.0	1.396	4.410	1.239	112.021	
	3.0	1.496	9.687	2.880	123.256	
	4.0	1.596	16.770	5.270	134.491	
	5.0	1.696	25.504	8.457	145.726	
	6.0	1.796	35.752	12.492	156.961	

Model	Towers				Cables
	Area A (m ²)	Torsional const. J (m ⁴)	Moment of inertia I_y (m ⁴) I_z (m ⁴)		Area A (10 ⁻² m ²)
600 m	1.114	12.935	7.067	10.915	1.439-2.686
900 m	1.434	28.061	15.984	22.380	1.532-2.825
1200 m	1.754	51.788	30.316	39.900	1.624-3.056

box shapes, respectively. The width of girders is assumed to be 30 m and the thickness of the flange and web of the girders is assumed to be 20 mm. The thickness of the towers is assumed to be 40 mm for all numerical models of the cable-stayed bridges. The yield strength of the steel for girders and towers is 450 MPa. The yield strength of cables for all numerical models is 1600 MPa. In addition, the depth of girders varies from 1.0 m to 6.0 m in order to investigate the effect of the girder depth on the ultimate load capacity of the cable-stayed bridges.

3.2 Loadings

Dead loads and design live loads are applied to the numerical models of the bridges. Dead loads include the self-weight of the components, initial cable forces and pedestrian loads. Because actual sections of girders and towers are idealized as simple 4-cell boxes sections and 1-cell box sections, the magnification factor 1.4 for dead loads is introduced in order to consider diaphragms and other utilities (Iwasaki *et al.* 2001). Dead loads for girders and towers are calculated as

$$w_G = 1.4A_G\gamma_s + 60.0 \tag{7}$$

$$w_T = 1.4A_T\gamma_s \tag{8}$$

where A_G and A_T are the section areas of girders and towers. γ_s is the unit-weight of steel and has a value of 76.98 kN/m³. The value 60.0 represents the weight of other structural elements and nonstructural elements such as pavement, street lamps and other attachments. Table 3 shows

Table 3 Detailed information of applied loads

Load type	Contents	Notes
Dead loads	Self weight	Girders, towers and cables
	Initial cable forces	Shape iterations with zero-displacement conditions
	Additional loads	Pavement, street lamps and other attachments
		Section magnification factor=1.4
		Equivalent elastic modulus
		60.0 kN/m
Live loads	Design live loads	lane loads according to the width of girders

Table 4 Dead loads and live loads

Models	Dead loads			Live loads L (kN/m)
	Girders		Towers	
	H (m)	w_G (kN/m)	w_T (kN/m)	
600 m	1.0	199.67		
	2.0	210.45	120.06	
	3.0	221.23		
900 m	4.0	232.00	154.55	76.20
	5.0	242.78		
1200 m	6.0	253.56	189.03	

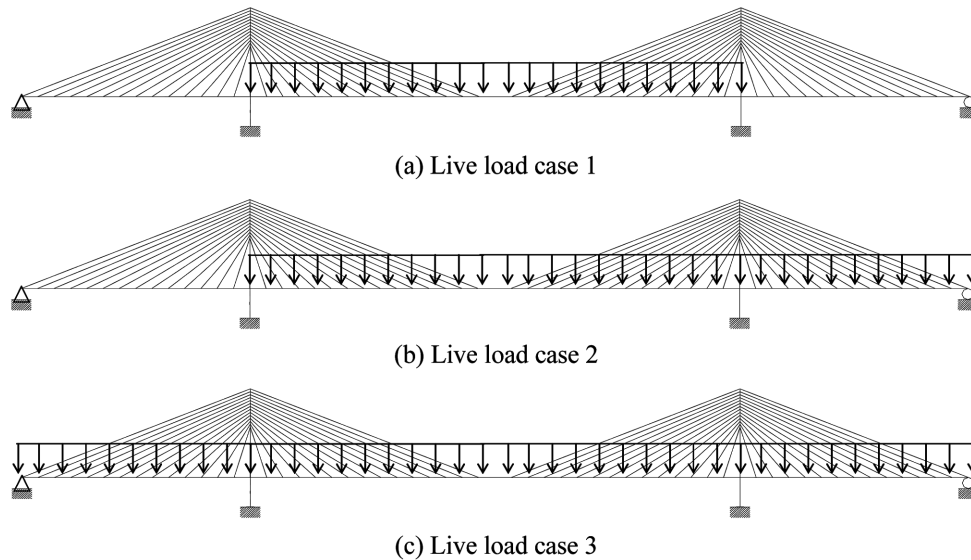


Fig. 11 Live load cases for cable-stayed bridges

detailed load information. Uniform lane load is applied to the numerical models as a live load and is based on the width of the girders. Three live load cases are considered in this study. First, uniform lane load is applied to the center span only (Load case 1). Second, uniform lane load is applied to the center span and one side of span (Load case 2). Finally, uniform lane load is applied to all spans (Load case 3). Table 4 shows the calculated values of dead loads and live loads. In addition, Fig. 11 presents three live load cases considered in this study.

4. Analysis results

4.1 Ultimate load capacity of the cable-stayed bridges

Numerical models of the cable-stayed bridges with center spans of 600 m, 900 m and 1200 m were analyzed with three live load cases using elastic buckling analysis, inelastic buckling analysis and nonlinear elasto-plastic analysis. For an illustration, numerical models of the cable-stayed bridges with a girder depth of 3 m are chosen to discuss results of the analysis. Buckling mode shapes by elastic and inelastic buckling analyses are plotted in Table 5~Table 7.

The minimum eigenvalues by elastic buckling analysis were calculated at a the value of 17.53 for live load case 1, 17.08 for live load case 2 and 17.09 for live load case 3, respectively for the models which have a center span of 600 m. The cable-stayed bridge has a structural margin more than 17 times the current design load by elastic buckling analysis. In the case of inelastic buckling analysis, however, the converged eigenvalues are calculated at a value of 5.22, 5.12 and 5.10 for three live load cases, respectively. Therefore, we concluded that the ultimate load capacity of cable-stayed bridges is greatly influenced by the inelastic material behavior of girders and towers. In addition, Table 5 shows that the buckling occurs at the center span in elastic buckling analysis, whereas it occurs at the tower and the intersection between girders and towers in inelastic buckling

analysis. Since the large axial force is concentrated at lower parts of the towers and the intersection between girders and towers, the components of a bridge near of these locations is susceptible to the buckling. Therefore, the buckling eigenmodes of inelastic buckling analysis is more realistic and reasonable than the ones of elastic buckling analysis.

Similar trends are shown for 900-m models and 1200-m models in Table 6 and Table 7. The minimum eigenvalues by elastic buckling analysis are quite different from the converged eigenvalues by inelastic buckling analysis. Elastic buckling analysis evaluates the overall safety of cable-stayed bridges as about 9 times (900-m models) and 5.5 times (1200-m models) that of design loads, whereas inelastic buckling analysis evaluates safety as only about 3.4 times (900-m models) and 2.6 times (1200-m models) that of current design loads. It is obvious that elastic buckling analysis greatly overestimates the overall safety of cable-stayed bridges. In addition, Table 6 and

Table 5 Buckling mode shapes of cable-stayed bridges (center span of 600 m and girder depth of 3 m)

Live load Cases	Elastic buckling analysis	Inelastic buckling analysis
Case 1	 $\kappa_{\min} = 17.53$	 $\kappa_{\min}^{conv} = 5.22$
Case 2	 $\kappa_{\min} = 17.08$	 $\kappa_{\min}^{conv} = 5.12$
Case 3	 $\kappa_{\min} = 17.09$	 $\kappa_{\min}^{conv} = 5.10$

Table 6 Buckling mode shapes of cable-stayed bridges (center span of 900 m and girder depth of 3 m)

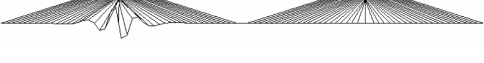
Live load Cases	Elastic buckling analysis	Inelastic buckling analysis
Case 1	 $\kappa_{\min} = 8.92$	 $\kappa_{\min}^{conv} = 3.45$
Case 2	 $\kappa_{\min} = 8.66$	 $\kappa_{\min}^{conv} = 3.39$
Case 3	 $\kappa_{\min} = 8.66$	 $\kappa_{\min}^{conv} = 3.38$

Table 7 Buckling mode shapes of cable-stayed bridges (center span of 1200 m and girder depth of 3 m)

Live load Cases	Elastic buckling analysis	Inelastic buckling analysis
Case 1	 $\kappa_{\min} = 5.60$	 $\kappa_{\min}^{conv} = 2.59$
Case 2	 $\kappa_{\min} = 5.52$	 $\kappa_{\min}^{conv} = 2.59$
Case 3	 $\kappa_{\min} = 5.51$	 $\kappa_{\min}^{conv} = 2.57$

Table 7 show that inelastic buckling analysis can describes the buckling behavior of main components in cable-stayed bridges, which occurs at the intersection between girders and towers where the large axial force is concentrated. It can also be seen that there are some asymmetries in buckling modes in Tables 5-7 although the geometries of overall bridge models are symmetric for left and right spans. Since the support conditions are not symmetric in bridge models as shown in Fig. 9, the initial cable forces and internal force distributions are slightly different for members in the left and right spans. It is probable that the asymmetries of buckling modes are due to these asymmetries of internal force distributions.

Figs. 12-14 show the distribution of the tangent modulus of the girders and towers for 600-m, 900-m and 1200-m models with the girder depth 3 m under live load case 3. It can be seen that the

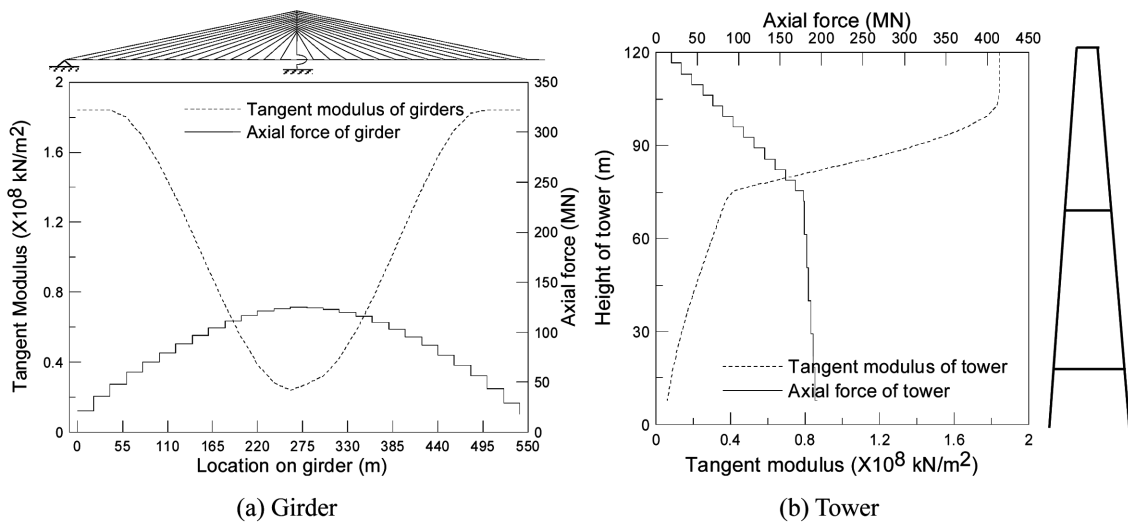


Fig. 12 Distribution of the tangent modulus of the girder and tower for 600-m model (Girder depth=3 m).

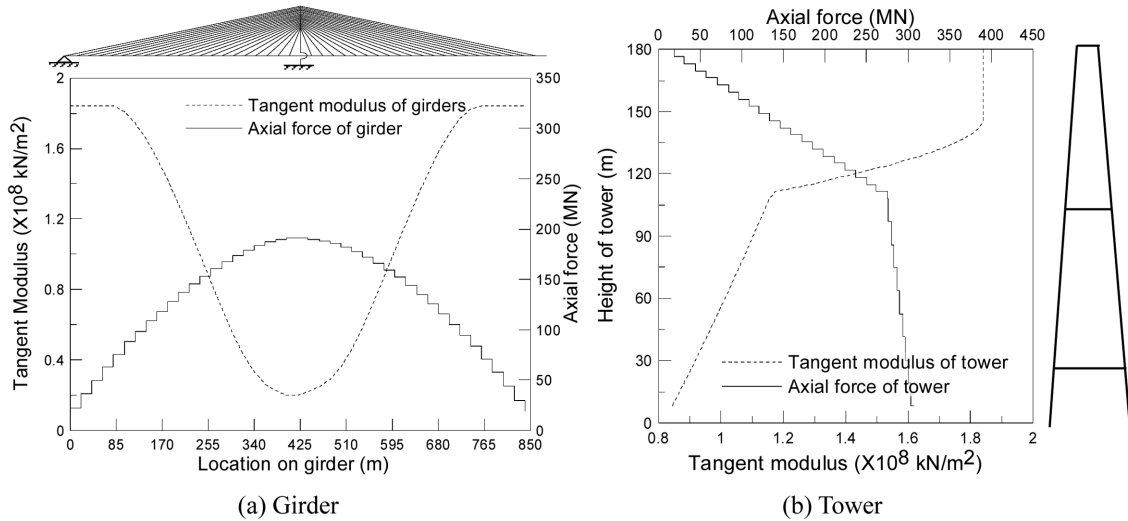


Fig. 13 Distribution of the tangent modulus of the girder and tower for 900-m model (Girder depth=3 m)

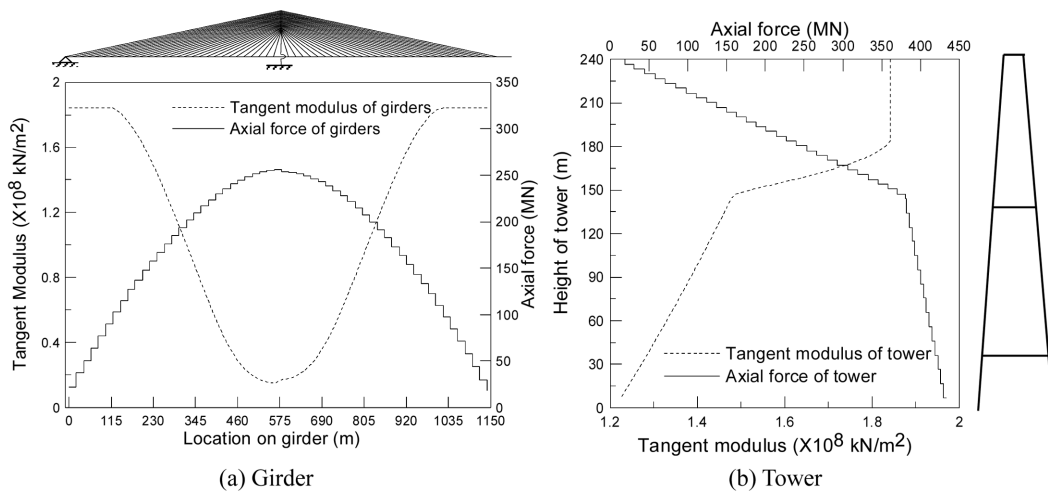
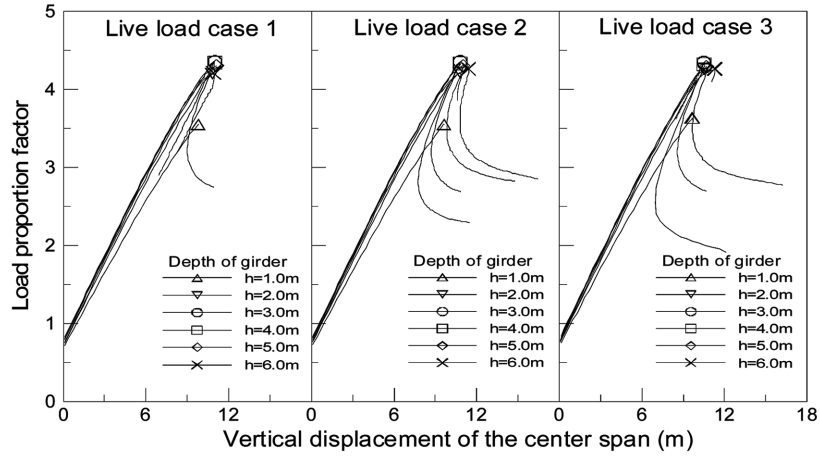


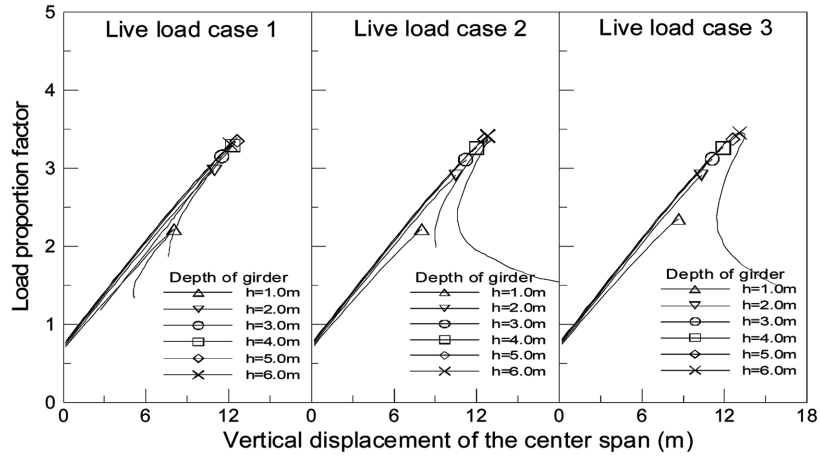
Fig. 14 Distribution of the tangent modulus of the girder and tower for 1200-m model (Girder depth=3 m)

tangent modulus is dramatically reduced for the members that have a large axial force (e.g. at the intersection between the girder and tower, the bottom of tower), whereas the modulus remain an elastic value for the members that have a small axial force (e.g. at girders at side supports and the center). These trends seem to be adequate to reflect the true inelastic behavior of the members in girders and towers of the bridge because the members that have large axial force will be firstly yielded at the critical stage of the bridge, whereas other members will be in elastic region.

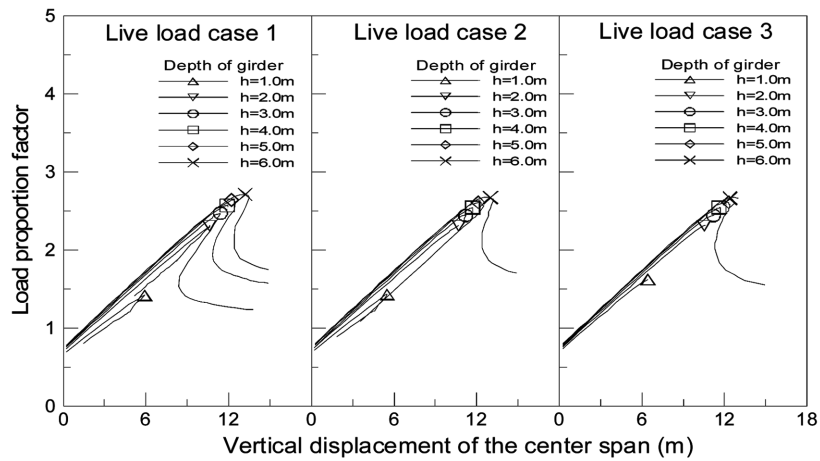
Load and displacement curves of nonlinear elasto-plastic analysis are plotted in Fig. 15 for all numerical models with three live load cases. The observation point and corresponding degree of freedom are selected at the center span and vertical displacement of the girder, respectively. Horizontal and vertical axes in Fig. 15 indicate the vertical displacement of the center span and load



(a) Center span of 600 m



(b) Center span of 900 m



(c) Center span of 1200 m

Fig. 15 Load-displacement curves of cable-stayed bridges

Table 8 Comparison of the ultimate load capacities by three computational methods

Model	Depth of girders	Elastic buckling analysis (minimum eigenvalue)			Inelastic buckling analysis (converged eigenvalue)			Elasto-plastic analysis (CLPF)		
		Case 1	Case 2	Case 3	Case 1	Case 2	Case 3	Case 1	Case 2	Case 3
600 m	1 m	4.88	4.89	5.09	4.00	4.01	4.12	3.55	3.55	3.63
	2 m	11.30	10.97	10.98	5.12	5.05	5.03	4.20	4.21	4.37
	3 m	17.53	17.08	17.09	5.22	5.12	5.10	4.35	4.35	4.60
	4 m	23.26	22.77	22.79	5.06	4.98	4.97	4.34	4.33	4.71
	5 m	28.76	28.54	28.58	4.92	4.86	4.85	4.30	4.30	4.29
	6 m	31.18	31.06	31.13	4.78	4.74	4.73	4.21	4.26	4.26
900 m	1 m	2.57	2.58	2.58	2.27	2.27	2.27	2.22	2.22	2.35
	2 m	5.80	5.63	5.64	3.19	3.13	3.12	2.97	2.91	2.91
	3 m	8.92	8.66	8.66	3.45	3.39	3.38	3.15	3.11	3.12
	4 m	11.90	11.59	11.59	3.61	3.56	3.55	3.29	3.26	3.26
	5 m	14.95	14.62	14.63	3.74	3.69	3.68	3.35	3.37	3.37
	6 m	17.62	17.41	17.46	3.84	3.83	3.82	3.31	3.41	3.45
1200 m	1 m	1.75	1.74	1.75	1.57	1.57	1.59	1.42	1.43	1.45
	2 m	3.50	3.50	3.61	2.36	2.36	2.38	2.31	2.31	2.31
	3 m	5.60	5.52	5.51	2.59	2.59	2.57	2.47	2.44	2.44
	4 m	7.57	7.44	7.43	2.70	2.69	2.67	2.57	2.54	2.54
	5 m	9.50	9.35	9.34	2.79	2.78	2.76	2.64	2.61	2.61
	6 m	11.34	11.17	11.16	2.86	2.85	2.84	2.71	2.67	2.66

proportion factor of the overall cable-stayed bridge, respectively. The location of critical points is designated as specific symbols for different depth of girders.

The critical load proportion factors of 600-m models with different girder depth are nearly the same except for the case of the girder depth of 1 m. After the initial yielding occurs at the lower parts of towers, the yielding spreads to the girders near of the intersection between girders and towers. Backstay cables and some intermediate cables yield at the ultimate stage in 600-m models.

In contrast, the yielding occurs initially at the girders near of the intersection between girders and towers in 900-m models. As the load increases, the yielding spreads to the lower parts of the towers and backstay cables. Similar trends are shown in 1200-m models. It is also noted that the ultimate load capacity of a bridge decreases as the center span increases. It is because that the cable-stayed bridge becomes more flexible and tends to have larger displacements as the center span increases; thus larger axial forces and moments occur at each element in comparably long-span bridges.

The indicators of ultimate load capacity for all models by three methods are summarized in Table 8. As can be seen in Table 8, the eigenvalues by elastic buckling analysis are quite different from the converged eigenvalues by inelastic buckling analysis and the critical load proportion factors by elasto-plastic analysis for all models of cable-stayed bridges. The reason for this phenomenon is that elastic buckling analysis cannot consider both the geometric nonlinearities and the inelastic material behavior of cable-stayed bridges. Obviously, the eigenvalues by elastic buckling analysis are invalid for the indicators of the ultimate load capacity of cable-stayed bridges since elastic buckling analysis greatly overestimates the overall safety of cable-stayed bridges.

In contrast, the converged eigenvalues by inelastic buckling analysis show good agreement with the critical load proportion factors by nonlinear elasto-plastic analysis for all numerical models, although geometric nonlinearities of cable-stayed bridges cannot be considered in inelastic buckling analysis. Consequently, it is concluded that the ultimate load capacity of cable-stayed bridges is largely affected by the inelastic material behavior rather than the geometric nonlinearities. In addition, inelastic buckling analysis is a good approximation for evaluation of the ultimate load capacity of cable-stayed bridges.

4.2 Effect of girder depth and live load cases on the ultimate load capacity

The ultimate load capacities of the cable-stayed bridges with different girder depths are presented in Fig. 16. The horizontal axis in Fig. 16 indicates girder depths, and the vertical axis indicates the converged eigenvalues or the critical load proportion factors of cable-stayed bridges. Since numerical results by elastic buckling analysis are quite different with those by other two methods, they are excluded from Fig. 16.

Fig. 16(a) shows that the ultimate load capacities of 600-m models increase until the depth of girder reaches 3 m in both analyses. However, they are almost unchanged in nonlinear elasto-plastic analysis and even decrease slightly in inelastic buckling analysis for the depth of girders larger than 3 m. It is probably because the dead load increments cancel out the capacity increments of a bridge,

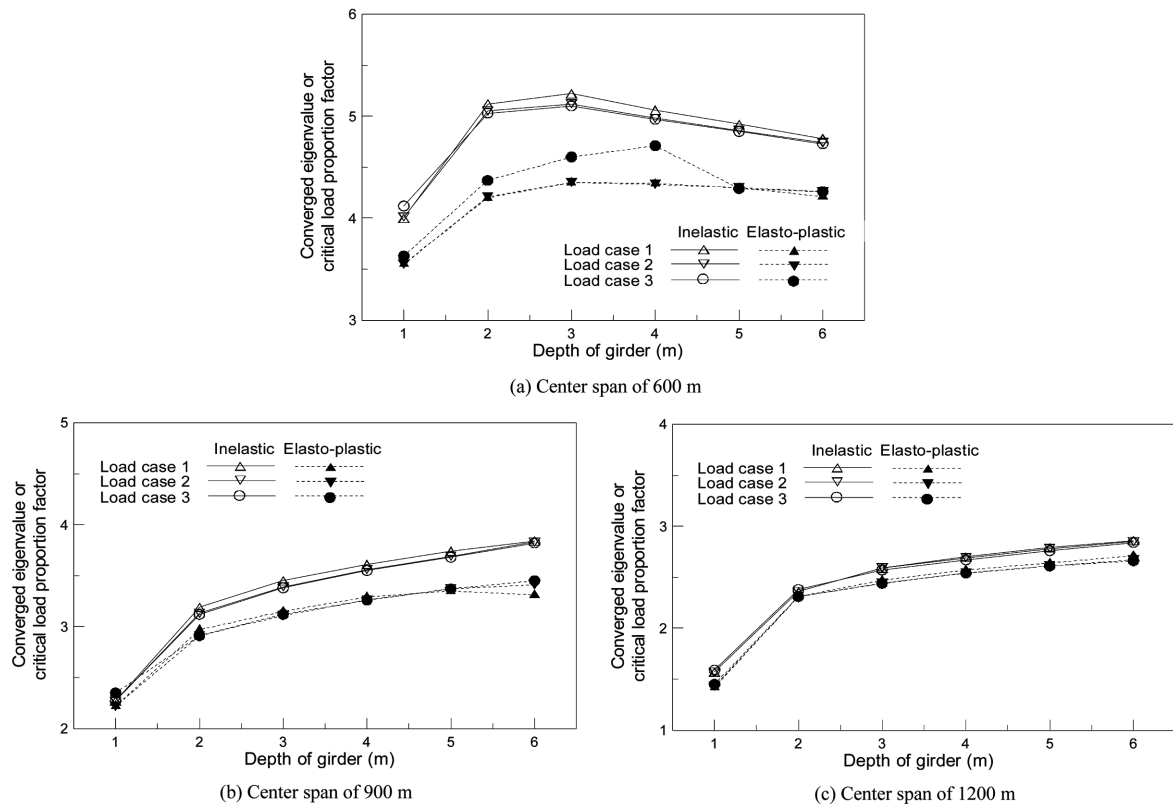
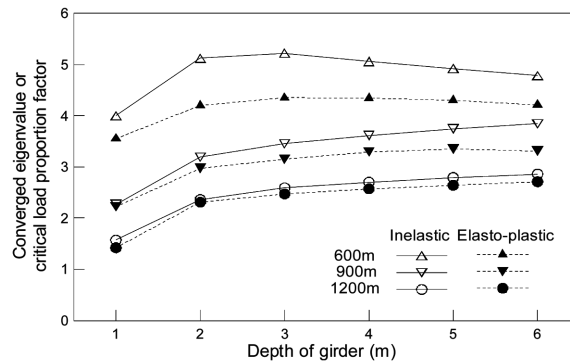


Fig. 16 Ultimate load carrying capacity trends with different live load cases

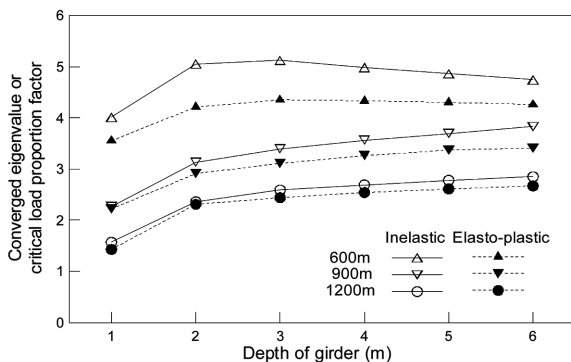
which are induced from increasing the stiffness of girders. Therefore, the most effective depth of girders can be selected at the range of 2-3 m in 600-m models. In addition, the differences among the ultimate load capacities with three live load cases are negligible in inelastic buckling analysis, whereas live load case 3 is more conservative than other two live load cases in nonlinear elasto-plastic analysis. As can be seen in Fig. 16(a), inelastic buckling analysis well describes the trends of the ultimate load capacity with different girder depths by nonlinear elasto-plastic analysis in 600-m models. The error between two analyses is 10% on the average and not exceeds 15%.

Fig. 16(b) shows that the ultimate load capacities of 900-m models gradually increase proportionally to the depth of girder in both analyses. However, a rate of increment of ultimate load capacity is almost negligible for the depth of girder larger than 4 m. Since the ultimate load capacities with three live load cases are nearly the same in 900-m models, it is concluded that live load cases are not important in 900-m models and there is no need to consider specific live load cases for the purpose of evaluation of ultimate load capacity. Ultimate load capacities by inelastic buckling analysis are in good agreement with nonlinear elasto-plastic analysis. The error between two analyses is 8% on the average for all depth ranges of girders.

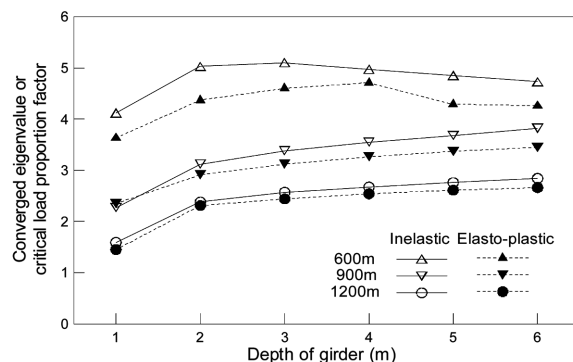
Similar trends are shown in 1200-m models as can be seen in Fig. 16(c). It is evident that a girder depth larger than 4 m has little effect on the ultimate load capacity of a comparably long span cable-stayed bridge. It is also noted that the error between two analyses is minimized in 1200-m models among all numerical models of cable-stayed bridges and 5% on the average.



(a) Live load case 1



(b) Live load case 2



(c) Live load case 3

Fig. 17 Ultimate load carrying capacity trends with different center spans

4.3 Validity and applicability of methods

Fig. 17 presents the ultimate load capacities by inelastic buckling analysis and nonlinear elasto-plastic analysis with different center spans. Horizontal axis in Fig. 17 indicates the depth of girders, and the vertical axis indicates the converged eigenvalues or the critical load proportion factors of cable-stayed bridges.

As shown in Fig. 17, errors of inelastic buckling analysis to nonlinear elasto-plastic analysis range from -15% to 3% for all numerical models of cable-stayed bridges. Inelastic buckling analysis can predict accurate ultimate load capacity of cable-stayed bridges, especially in long span bridges that have a center span of 1200 m. For these models, errors in inelastic buckling analysis reduce to below 5%. Nonlinear elasto-plastic analysis is inefficient for the practical design of cable-stayed bridges because of its theoretical complexity and lengthy calculation time. Inelastic buckling analysis used in this study is quite simple to use compared to nonlinear elasto-plastic analysis. Fast computation time is an additional advantage of inelastic buckling analysis. It is obvious that inelastic buckling analysis is faster than nonlinear elasto-plastic analysis since there is no need to solve algebraic equations repeatedly. Consequently, inelastic buckling analysis is a simple approximation method for evaluation of ultimate load capacity of a long span cable-stayed bridge.

5. Conclusions

In this paper, the indicators for ultimate load capacity of cable-stayed bridges are defined by the methods of elastic buckling analysis, inelastic buckling analysis and nonlinear elasto-plastic analysis. The algorithm for inelastic buckling analysis is presented and corresponding computer codes were developed. In order to consider inelastic material behavior, the column strength curves prescribed in AASHTO LRFD specifications were used. In addition, nonlinear elasto-plastic analysis is performed using the proprietary software ABAQUS. User subroutines in ABAQUS are newly written in order to consider nonlinear behavior for the cable sag effect. Ultimate load capacities are calculated for numerical models of cable-stayed bridges that have center spans of 600 m, 900 m and 1200 m. The effect of the girder depth and live load cases were investigated. We present the following conclusions:

1. Elastic buckling analysis is invalid for evaluation of the ultimate load capacity of cable-stayed bridges since it cannot consider both geometric nonlinearities and inelastic material behavior; thus it greatly overestimates overall safety of cable-stayed bridges.
2. Inelastic buckling analysis is an effective approximation method for evaluation of the ultimate load capacity of long span cable-stayed bridges because of the efficiency of computation time and simplicity of application.
3. The ultimate load capacity of cable-stayed bridges is mainly affected by inelastic material behavior rather than geometric nonlinearities since inelastic buckling analysis, which cannot consider geometric nonlinearities, shows good agreement with nonlinear elasto-plastic analysis.
4. For evaluation of ultimate load capacity, the errors between inelastic buckling analysis and nonlinear elasto-plastic analysis range from -15% to 3%. The errors in inelastic buckling analysis are 10% on the average in 600-m models, whereas they reduce to below 5% in 1200-m models. Consequently, inelastic buckling analysis can predict accurate ultimate load capacity of cable-stayed bridges, especially in long span bridges.

Acknowledgements

This work is a part of a research project supported by Korea Ministry of Construction & Transportation (MOCT) through Korea Bridge Design & Engineering Research Center. The authors wish to express their gratitude for the financial support.

References

- AASHTO (2004), *LRFD Bridge Design Specifications*, American Association of State Highway and Transportation Officials, Third Edition.
- Adeli, H. and Zhang, J. (1995), "Fully nonlinear analysis of composite girder cable-stayed bridges", *Comput. Struct.*, **54**(2), 267-277.
- Engesser, F. (1889) "Ueber die Knickfestigkeit Gerader Stäbe", *Zeitschrift für Architektur und Ingenieurwesen*, **35**, 455 (in German).
- Ermopoulos, J.C., Vlahino, A.S. and Wang, Y.C. (1992), "Stability analysis of cable-stayed bridges", *Comput. Struct.*, **44**(5), 1083-1089.
- Ernst, J.H. (1965), "Der E-Modul von seilen unter berucksichtigung des Durchchanges", *Der Bauingenieur*, **40**(2), 52-55 (in German).
- George, H.W. (1999), "Influence of deck material on response of cable-stayed bridges to live loads", *J. Bridge Eng.*, ASCE, **4**(2), 136-142.
- Gimsing, N.J. (1983), *Cable-Supported Bridges, Concept and Design*. Wiley, Chichester.
- Iwasaki, H., Nogami, K. and Nagai, M. (2001), "Precision of E_f method for evaluating load-carrying capacity of long-span cable-stayed bridges and its ultimate strength check", *IABSE Conference*, IABSE reports, Seoul, **84**, 110-111.
- Kanok-Nukulchai, W. and Hong, G. (1993), "Nonlinear modelling of cable-stayed bridges", *J. Constr. Steel Res.*, **26**(2/3), 249-266.
- Karoumi, R. (1999), "Some modeling aspects in the nonlinear finite element analysis of cable-supported bridges", *Comput. Struct.*, **71**, 397-412.
- McGuire, W., Gallagher, R.H. and Ziemian, R.D. (2000), *Matrix Structural Analysis*, 2nd Edition, John Wiley & Sons, New York.
- Nagai, M., Fujino, Y., Yamaguchi, H. and Iwasaki, E. (2004), "Feasibility of a 1400 m span steel cable-stayed bridge", *J. Bridge Eng.*, ASCE, **9**(5), 444-452.
- Poldony, W.J. and Scalzi, J.B. (1976), *Construction and Design of Cable-Stayed Bridge*. Wiley, New York.
- Ren, W.X. (1999), "Ultimate behavior of long-span cable-stayed bridges", *J. Bridge Eng.*, ASCE, **4**(1), 30-37.
- Shu, H.S. and Wang, Y.C. (2001), "Stability analysis of box-girder cable-stayed bridges", *J. Bridge Eng.*, ASCE, **6**(1), 63-68.
- Tang, M.C. (1976), "Buckling of cable-stayed bridges", *J. Struct. Div.*, ASCE, **102**(9), 1675-1684.
- Wang, Y.C. (1999), "Number of cable effects on buckling analysis of cable-stayed bridges", *J. Bridge Eng.*, ASCE, **4**(4), 242-248.
- Wang, P.H., Lin, H.T. and Tang, T.Y. (2002), "Study on nonlinear analysis of a highly redundant cable-stayed bridge", *Comput. Struct.*, **80**, 165-182.
- Xi, Y. and Kuang, J.S. (2000), "An energy approach for geometrically non-linear analysis of cable-stayed bridges", *Proc. of the Institution of Civil Engineers-Structures and Buildings*, **140**, 227-237.
- Xi, Y. and Kuang, J.S. (1999), "Ultimate load capacity of cable-stayed bridges", *J. Bridge Eng.*, ASCE, **4**(1), 14-22.
- Yang, Y.B. and Kuo, S.R. (1994), *Theory and Analysis of Framed Structures*, Prentice Hall, Singapore.